Trialkylphosphine-Stabilized Copper−Phenyltellurolate Complexes: From Small Molecules to Nanoclusters via Condensation Reactions

Marty W. DeGroot, Michael W. Cockburn, Mark S. Workentin, and John F. Corrigan*

Department of Chemistry, The University of Western Ontario, London, Ontario, N6A 5B7 Canada

Received November 14, 2000

Reactions of CuCl with $Te(Ph)SiMe_3$ and solublizing trialkylphosphine ligands afford a series of polynuclear copper−phenyltellurolate complexes that has been structurally characterized. The formation of the complexes is found to be highly dependent on the ancillary phosphine ligand used. The synthesis and structures of $[Cu_2(\mu\text{-}TePh)_2(PMe_3)_4]$ **1**, $[Cu_4(\mu_3\text{-}TePh)_4(PPr^i_3)_3]$ **2**, $[Cu_5(\mu\text{-}TePh)_3(\mu_3\text{-}TePh)_3(PEt_3)_3][PEt_3Ph]$ **3**, and $[Cu_{12}Te_3(\mu_3\text{-}TePh)_6(PEt_3)_6]$ **4** are described. The telluride (Te^{2-}) ligands in **4** arise from the generation of $TePh_2$ in the reaction mixtures. The subsequent co-condensation of clusters **3** and **4** leads to the generation of the nanometer sized complex $[Cu_{29}Te_9(\mu_3\text{-}TePh)_{10}(\mu_4\text{-}TePh)_2(PEt_3)_8][PEt_3Ph]$ **5** in good yield, in addition to small amounts of $[Cu_{39}(\mu_3\text{-}TePh)_{10}(\mu_4\text{-}TePh)Te_{16}(PEt_3)_{13}]$ **6**. These complexes are formed via the photo elimination of $TePh_2$. The cyclic voltammogram of **5** in THF solution exhibits two oxidation waves, assigned to the oxidation of the Cu(I) centers.

Introduction

The chemistry of metal−selenolate and metal−tellurolate polynuclear (cluster) complexes continues to attract considerable attention. The demonstrated ability of the heavier chalcogenolate ligands, either alone or in conjunction with other (eg. phosphine) ligands, to stabilize a variety of skeletal geometries is making them an increasingly important method for binary nanocluster synthesis.[1] Despite the surge in the development of this area of chemistry, the synthesis and structural characterization of nanoscale metal−tellurium cluster complexes[2] remains underdeveloped relative to their selenium congeners. This may be attributed, in part, to the instability and difficulty of handling $Te(SiMe_3)_2$ compared to $Se(SiMe_3)_2$, the latter reagent finding widespread use as an excellent source of Se^{2-} in the synthesis of metal−selenide nanoclusters and colloids.[3] Steigerwald and co-workers have demonstrated the utility of trialkylphosphine tellurides ($R_3P{=}Te$) as a source of soluble "Te(0)" to form numerous high-nuclearity, metal−telluride polynuclear complexes, when treated with suitable metal(0) reagents.[2c−f]

It has been demonstrated that metal−chalcogenolate $M(ER)_x$ complexes can be used as single source precursors to binary solid-state materials via the elimination of ER_2.[4] Arnold and co-workers also demonstrated that the Lewis base-induced elimination of TeR_2 from homoleptic metal−tellurolates leads to the formation of metal−telluride complexes.[5] We demonstrated that photochemical-induced condensation reactions of phosphine-stabilized copper−tellurolate cluster can lead to the generation of higher nuclearity complexes[6] and recent work by Fenske and co-workers illustrated the general applicability of using arylselenolate ligands to effectively stabilize copper−

(1) (a) Eichhöfer, A.; Fenske, D. *J. Chem. Soc., Dalton Trans.* **2000**, 941−944. (b) Corrigan, J. F.; Fenske, D. *Chem. Commun.* **1996**, 943−944. (c) Bettenhausen, M.; Fenske, D. *Z. Anorg. Allg. Chem.* **1998**, *624*, 1245−1246. (d) Behrens, S.; Bettenhausen M.; Eichhöfer, A.; Fenske, D. *Angew Chem. Int. Ed. Engl.* **1997**, *36*, 2797−2799. (e) Behrens, S.; Fenske, D. *Ber. Bunsen Phys. Chem.* **1997**, *101*, 1588−1592. (f) Behrens, S.; Bettenhausen, M.; Deveson, A. C.; Eichhöfer, A.; Fenske, D.; Lohde, A.; Woggon, U. *Angew. Chem., Int. Ed. Engl.* **1996**, *35*, 2215−2218. (g) Freedman, D.; Emge, T. J.; Brennan, J. G. *J. Am. Chem. Soc.* **1997**, *119*, 11112−11113. (h) Lee, G. S. H.; Fisher, K. J.; Craig, C.; Scudder, M. L.; Dance, I. G. *J. Am. Chem. Soc.* **1990**, *112*, 6435−6437.

(2) (a) Eichhöfer, A.; Corrigan, J. F.; Fenske, D.; Tröster, E. *Z. Anorg. Allg. Chem.* **2000**, *626*, 338−348. (b) Fenske, D.; Steck, J.-C. *Angew. Chem., Int. Ed. Engl.* **1993**, *32*, 238−242. (c) Steigerwald, M. L. *Polyhedron* **1994**, *13*, 1245−1252. (d) Steigerwald, M. L.; Siegrist, Stuczynski, S. M. *Inorg. Chem.* **1991**, *30*, 4940−4945. (e) Brennan, J. G.; Siegrist, T.; Stuczynski, S. M.; Steigerwald, M. L. *J. Am. Chem. Soc.* **1990**, *112*, 9233−9236. (f) Brennan, J. G.; Siegrist, T.; Stuczynski, S. M.; Steigerwald, M. L. *J. Am. Chem. Soc.* **1989**, *111*, 9240−9242. (g) Eichhöfer, A.; Fenske, D.; Pfistner, H.; Wunder, M. *Z. Anorg. Allg. Chem.* **1998**, *624*, 1909−1914. See also Dance, I. G.; Fisher, K. *Prog. Inorg. Chem.* **1994**, *41*, 637−803. Roof, L. C.; Kolis, J. W. *Chem. Rev.* **1993**, *93*, 1037−1080.

(3) (a) Steigerwald, M. L.; Alivisatos, A. P.; Gibson, J. M.; Harris, T. D.; Kortan, R.; Muller, A. J.; Thayer, A. M.; Duncan, T. M.; Douglass, D. C.; Brus, L. E. *J. Am. Chem. Soc.* **1988**, *110*, 3046−3050. (b) Murray, C. B.; Norris, D. J.; Bawendi, M. G. *J. Am. Chem. Soc.* **1993**, *115*, 8706−8715. (c) Eichhöfer, A.; Fenske, D. *J. Chem. Soc., Dalton Trans.* **1998**, 2969−2972. (d) Krautscheid, H.; Fenske, D.; Baum, G.; Semmelmann, M. *Angew Chem. Int. Ed. Engl.* **1993**, *32*, 1303−1305. (e) Deveson, A.; Dehnen, S.; Fenske, D. *J. Chem. Soc., Dalton Trans.* **1997**, 4491−4497. (f) Fenske, D.; Krautscheid, H.; Balter, S. *Angew. Chem., Int. Ed. Engl.* **1990**, *29*, 796−799.

(4) (a) Steigerwald, M. L.; Sprinkle, C. R. *J. Am. Chem. Soc.* **1987**, *109*, 7200−7201. (b) O'Brien, P. *Chemtronics* **1991**, *5*, 61−70. (c) Steigerwald, M. L.; Sprinkle, C. R. *Organometallics* **1988**, *7*, 245−246. (d) Singh, H. K; Sudha, N. *Polyhedron* **1996**, *15*, 745−763. (e) Steigerwald, M. L.; Siegrist, T.; Stuczynski, S. M. *Inorg. Chem.* **1991**, *30*, 2256−2257. (f) Brennan, J. G.; Siegrist, T.; Carroll, P. J.; Stuczynski, S. M.; Brus, L. E.; Steigerwald, M. L. *J. Am. Chem. Soc.* **1989**, *111*, 4141−4143. (g) Strzelecki, A. R.; Timinski, P. A.; Helsel, B. A.; Bianconi, P. A. *J. Am. Chem. Soc.* **1992**, *114*, 3159−3160. (h) Strzelecki, A. R.; Likar, C. L.; Helsel, B. A.; Utz, T.; Lin, M. C.; Bianconi, P. A. *Inorg. Chem.* **1994**, *33*, 5188−5194. (i) O'Brien, P.; Nomura, R. *J. Mater. Chem.* **1995**, *5*, 1761−1773. (j) Steigerwald, M. L.; Rice, C. E. *J. Am. Chem. Soc.* **1988**, *110*, 4228−4231. (k) Bochmann, M. *Chem. Vap. Deposition* **1996**, *2*, 85−96. (l) Cheon, J. W.; Arnold, J.; Yu, K. M.; Bourret E. D. *Chem Mater.* **1995**, *7*, 2273−2276. (m) Stoll, S. L.; Barron, A. R. *Chem. Mater.* **1998**, *10*, 650−657. (n) Bochmann, M.; Webb, K.; Harman, M.; Hursthouse, M. B. *Angew. Chem., Int. Ed. Engl.* **1990**, *29*, 638−639. (o) Cheng, Y.; Emge, T.; Brennan, J. G. *Chem. Mater.* **1995**, *7*, 2273−2276.

(5) (a) Gerlach, C. P.; Christou, V.; Arnold, J. *Inorg. Chem.* **1996**, *35*, 2758−2766. (b) Christou, V.; Arnold, J. *J. Am. Chem. Soc.* **1992**, *114*, 6240−6242.

(6) Corrigan, J. F.; Fenske, D. *Angew. Chem., Int. Ed. Engl.* **1997**, *36*, 1981−1983.

10.1021/ic001260k CCC: $20.00
Published on Web 07/27/2001

selenide and silver−selenide "giant" clusters.[7] The ability of $E(R)^-$ and $E(Ar)^-$ ligands to bridge two, three, and even four metal centers has resulted in a wide variety of structural types being isolated and structurally characterized.

We wished to further probe facile condensation routes into high-nuclearity metal−telluride complexes starting with "low nuclearity" precursors. Herein we describe the synthesis and characterization of several phosphine-stabilized copper−phenyltellurolate complexes including two high-nuclearity copper−telluride clusters $[Cu_{29}(TePh)_{12}Te_9(PEt_3)_8][PEt_3Ph]$ **5** and $[Cu_{39}(TePh)_{11}Te_{16}(PEt_3)]$ **6**, formed from the co-condensation of the complexes $[Cu_{12}Te_3(TePh)_6(PEt_3)_6]$ **3** and $[Cu_5(TePh)_6(PEt_3)_3][PEt_3Ph]$ **4**.

Experimental Section

Standard Schlenk line and drybox techniques[8] were employed throughout with high-purity, dried nitrogen. Solvents for reactions and crystallizations were distilled under nitrogen from appropriate drying agents prior to use. Diethyl ether, tetrahydrofuran, hexane and pentane were dried over sodium/benzophenone. Trialkylphosphines[9a−c] and Te(Ph)$SiMe_3$[9d] were prepared by literature procedures. ^1H and $^{31}P\{^1H\}$-NMR spectra were obtained on a Varian Mercury 400 (operating frequencies 400.09 and 161.96 MHz, respectively) or Inova 400 (operating frequencies 399.76 and 161.83 MHz, respectively) spectrometer. ^1H spectra were referenced to residual protio impurities of the deuterated solvents, while $^{31}P\{^1H\}$ spectra were referenced externally to H_3PO_4. UV−vis spectra were recorded on a Varian Cary 100 spectrometer, scanning from 700 to 200 nm. Infrared spectra were recorded on a Nicolet Avatar 3200 FTIR spectrometer. Reported melting points are uncorrected. Chemical analyses were performed by Chemisar Laboratories (Guelph, Ontario) and the Institut für Anorganische Chemie, Karlsruhe, Germany.

Synthesis of $[Cu_2(TePh)_2(PMe_3)_4]$ 1. A total of 0.15 g (1.5 mmol) of CuCl and 0.31 mL (3.0 mmol) of PMe_3 were mixed in 5 mL of THF to form a clear solution. To the solution was added 0.35 mL (1.5 mmol) of Te(Ph)$SiMe_3$ to yield a yellow/pale green solution. The solution was stirred for 40 min and layered with hexane. Yellow crystals of **1** grew at room temperature within 2−3 days. Yield: 0.33 g (55%). Anal. Calcd for $C_{24}H_{46}P_4Cu_2Te_2$: C, 34.3; H, 5.51. Found: C, 34.6; H, 5.61. NMR (δ, C_6D_6): ^1H 8.32 (d, $J_{HH} = 7$ Hz, $4H_{phenyl}$), 7.00 (vt, $J_{HH} = 7$ Hz, $2H_{phenyl}$), 6.87 (vt, $J_{HH} = 7$ Hz, $4H_{phenyl}$), 0.91 (d, $J_{PH} = 4$ Hz, 36 H_{CH3}) ppm; $^{31}P\{^1H\}$ −44.5 (s, $W_{1/2} = 204$ Hz) ppm. Mp: 86° C (decomp). UV−vis (THF): broad featureless spectrum, with increasing absorbance from $\lambda_{onset} = 470$ nm. Selected IR data (KBr): 3045w, 2961m, 2925w, 1569m, 1469m, 1261s, 1096s, 1032s, 1015s, 802s.

Synthesis of $[Cu_4(TePh)_4(PPr^i_3)_3]$ 2. A total of 0.32 g (3.2 mmol) of CuCl was dissolved in 15 mL of Et_2O with 1.23 mL (6.5 mmol) of PPr^i_3. To the solution was added 0.75 mL (3.2 mmol) of Te(Ph)$SiMe_3$ to yield a bright yellow homogeneous solution. The solution was stirred for 5 min. The solvent was reduced by $\sim^1/_2$ in volume and bright yellow crystals of **2** grew within a few hours. Yield: 0.45 g (35%). Anal. Calcd for $C_{51}H_{83}P_3Cu_4Te_4$: C, 39.4; H, 5.38. Found: C, 39.4; H, 5.32. NMR (δ, C_6D_6): ^1H 8.11 (d, $J_{HH} = 7$ Hz, $8H_{phenyl}$), 6.99 (vt, $J_{HH} = 7$ Hz, $4H_{phenyl}$), 6.85 (vt, $J_{HH} = 7$ Hz, $8H_{phenyl}$), 1.89 (br s, $9H_{CH}$), 1.09 (mult, $54H_{CH3}$) ppm; $^{31}P\{^1H\}$ 20.6 (s, $W_{1/2} = 45$ Hz) ppm. Mp: 155 °C. UV−vis (THF): broad featureless spectrum, with increasing absorbance from $\lambda_{onset} = 460$ nm. Selected IR data (KBr): 3048w, 2952m, 1569m, 1467m, 1429m, 1291m, 1261w, 1092m, 1058s, 881m, 802s.

Synthesis of $[Cu_5(TePh)_6(PEt_3)_3][PEt_3Ph]$ 3 and $[Cu_{12}Te_3(TePh)_6(PEt_3)_6]$ 4. PEt_3 (0.49 mL, 3.3 mmol) was added to a suspension CuCl (0.33 g, 3.3 mmol) in pentane (20 mL) and stirred for 45 min. Te(Ph)$SiMe_3$ (0.93 mL, 4.0 mmol) was then added to yield a bright yellow, homogeneous solution. After stirring for 1 h, the yellow solution was allowed to stand undisturbed. The solution gradually darkened to a dark green in color and small, yellow-orange, needlelike crystals of **3** formed overnight. After a few more days, dark green, hexagonal prisms of **2** appeared. It was observed that the formation of these metal clusters seemed to proceed more quickly in the presence of direct sunlight. The crystals were isolated (0.22 g), washed with pentane and separated manually. Yield: **3** 0.09 g (8%, based on Cu) and **4** 0.13 g (15%, based on Cu). Anal. Calcd for $C_{66}H_{95}P_4Cu_5Te_6$: C, 37.8; H, 4.57. Found: C, 37.6; H, 5.15. Anal. Calcd for $C_{72}H_{120}P_6Cu_{12}Te_9$: C, 28.1; H, 3.92. Found: C, 28.5; H, 4.01. Data for **3** NMR (δ, C_6D_6): ^1H 8.19 (br s, 12 H_{phenyl}), 7.92, d, $J_{HH} = 7$ Hz, 2 H_{phenyl}), 7.06−6.78 (mult, 21 H_{phenyl}), 2.11 (dq, $J_{HH} = 7$ Hz, $J_{PH} = 12$ Hz, 6 H_{CH2}), 1.45 (br s, 18 H_{CH2}), 0.95 (br s, 27 H_{CH3}), 0.37 (dt, $J_{HH} = 7$ Hz, $J_{PH} = 19$ Hz, 9 H_{CH3}) ppm; $^{31}P\{^1H\}$ 35.5(s), −19.4 (br s, $W_{1/2} = 58$ Hz) ppm. Mp: 131 °C (decomp). UV−vis (THF): broad featureless spectrum, with increasing absorbance from $\lambda_{onset} = 470$ nm. Selected IR data ($CHCl_3$): 2963m, 1559m, 1472m, 1261s, 1205m, 1099s, 1016s, 800s. Data for **4** NMR (δ, C_6D_6): ^1H 8.17 (d, $J_{HH} = 8$ Hz, 12 H_{phenyl}), 7.06 (vt, $J_{HH} = 7$ Hz, $6H_{phenyl}$), 6.99 (vt, $J_{HH} = 7$ Hz, $12H_{phenyl}$), 1.33 (mult, $36H_{CH2}$), 0.92 (dt, $J_{HH} = 8$ Hz, $J_{PH} = 14$ Hz, $54H_{CH3}$) ppm; $^{31}P\{^1H\}$ −14.8 (br s, $W_{1/2} = 27$ Hz) ppm. Mp: 145−146 °C. UV−vis (THF): $\lambda_{max} = 640$, 440 nm. Selected IR data (KBr): 3046w, 2962m, 2925w, 1569m, 1469m, 1261s, 1097s, 1033s, 1015s, 802s.

Synthesis of $[Cu_{29}Te_9(TePh)_{12}(PEt_3)_8][PEt_3Ph]$ 5 and $[Cu_{39}(TePh)_{11}Te_{16}(PEt_3)_{13}]$ 6. Cluster $[Cu_{29}(TePh)_{12}Te_9(PEt_3)_8][PEt_3Ph]$ **5** was prepared from the co-condensation reaction of the two smaller clusters **3** and **4**. Cluster **3** (0.09 g, 0.043 mmol) and cluster **4** (0.19 g, 0.062 mmol) were dissolved in 6.5 mL THF to yield a dark green−yellow solution. The solution was stirred for 24 h and the resulting deep wine-red solution was then layered with diethyl ether via slow diffusion. After a few days, purple crystals of **5** formed. The solvent was removed and the crystals washed with two small portions of diethyl ether (10 mL). Yield: 42% (0.12 g). Crystals of **6** formed in the mother liquor after an additional 48−72 h (Yield: ∼ 2%). When this experiment was attempted in the absence of light, there was no evidence for the formation of **5** (or **6**). NMR analysis of the mother liquor confirmed the presence of $TePh_2$ in the reaction mixture. Anal. Calcd for $C_{132}H_{200}P_9Cu_{29}Te_{21}$: C, 24.1; H, 3.06. Found: C, 24.1; H, 3.22. Anal. Calcd for C_{144} $H_{250}P_{13}Cu_{39}Te_{27}$: C, 20.8; H, 3.03. Found: C, 19.0; H, 2.67; $^{31}P\{^1H\}$ NMR data for **5** (δ, C_6D_6/C_4H_8O): 38.1 (s), −15.6 (br s, $W_{1/2} = 145$ Hz), −18.3 (br s, $W_{1/2} = 175$ Hz) ppm. Mp: **5**, 171 °C (decomp); **6**, >300 °C. UV−vis data for **5** and **6** are discussed in the text. Selected IR data for **5** (KBr): 3046w, 2962m, 2923w, 1569m, 1469m, 1261s, 1097s, 1033s, 1015s, 802s. Selected IR data for **6** (KBr): 3043w, 2958m, 2927w, 1569m, 1469m, 1033m, 1015m, 766m, 727m.

Electrochemical Experiments. Cyclic voltammetry was performed using a PAR 263 potentiostat interfaced to a personal computer using PAR 270 electrochemistry software. The electrochemical cell was contained in an inert atmosphere glovebox at room temperature to prevent air and moisture contamination to the sample. In a typical experiment 1 or 2 mM of solute was added to dry THF solvent containing 0.1−0.2 M tetrabutylammonium tetrafluoroborate as the electrolyte. Prior to each experiment the working electrode, a 0.5 mm diameter platinum (Pt) electrode, was freshly polished with 1 μ diamond paste and ultrasonically cleaned in ethanol for fifteen minutes. The counter electrode was a platinum flag and the reference a silver wire immersed in a glass tube containing electrolyte in THF with a fine sintered ceramic bottom. Ferrocene was used as an internal redox reference, and thus the potentials can be referenced to the Ag/AgCl/KCl reference electrode: $Fc/Fc+ = 0.629$V.[10] To compensate for the cells internal resistance, the *iR* compensation was adjusted to at least 96% of the oscillation value.

(7) (a) Bettenhausen, M.; Eichöfer, A.; Fenske, D.; Semmelmann, M. *Z. Anorg. Allg. Chem.* **1999**, *625*, 593−601. (b) Zhu, N.; Fenske, D. *J. Chem. Soc., Dalton Trans.* **1999**, 1067−1075. (c) Fenske, D.; Zhu, N.; Langetepe; T. *Angew. Chem., Intl. Ed. Engl.* **1998**, *37*, 2640−2644.

(8) Errington, R. J. *Advanced Practical Inorganic and Metalorganic Chemistry*; Blackie Academic and Professional: London, 1997.

(9) (a) Sasse, K. In *Methoden der Organischen Chemie, Band 1*; Houben-Weyl, Ed.; Thieme Verlag: Stuttgart, 1963; p 32. (b) Kaesz, H. D.; Stone, F. G. A. *J. Org. Chem.* **1959**, *24*, 635−637. (c) Cumper, C. W. N.; Foxton, A. A.; Read, J.; Vogel, A. I. *J. Chem. Soc.* **1964**, 430−434. (d) Drake, J. E.; Hemmings, R. T. *Inorg. Chem.* **1980**, *19*, 1879−1883.

Table 1. Crystallographic Data for the Structure Determinations of $[Cu_2(TePh)_2(PMe_3)_4]$ **1**, $[Cu_4(TePh)_4(PPr^i_3)_3]$ **2**, $[Cu_5(TePh)_6(PEt_3)_3][PEt_3Ph]$ **3**, $[Cu_{12}Te_3(TePh)_6(PEt_3)_6]$ **4**, $[Cu_{29}Te_9(TePh)_{12}(PEt_3)_8][PEt_3Ph]$ **5**, and $[Cu_{39}Te_{16}(TePh)_{11}(PEt_3)_{13}]$ **6**

	1	**2**	**3**	**4**	**5**	**6**
chemical formula	$C_{24}H_{46}P_4Cu_2Te_2$	$C_{51}H_{83}P_3Cu_4Te_4$	$[C_{54}H_{75}P_3Cu_5Te_6][C_{12}H_{20}P]$	$C_{72}H_{120}P_6Cu_{12}Te_9$	$[C_{120}H_{180}Cu_{29}P_8Te_{21}][C_{12}H_{20}P]$	$C_{144}H_{250}P_{13}Cu_{39}Te_{27}$
formula weight	840.77	1553.64	2095.60	3082.38	6587.91	8307.31
temperature (°C)	−73	−73	−73	−73	−73	−73
space group	$P2_1/c$ (No. 14)	$P2_1/n$ (No. 14)	$P2_1/c$ (No. 14)	$P\bar{3}1c$ (No. 163)	$P2_1$ (No.4)	$P\bar{1}$ (No. 1)
a (Å)	17.528(4)	11.701(1)	17.480(1)	15.345(1)	19.830(3)	19.6195(2)
b (Å)	13.891(3)	20.502(2)	14.552(1)		18.193(2)	20.6286(3)
c (Å)	13.882(3)	25.555(3)	30.403(2)	24.412(2)	30.101(4)	32.1288(5)
α (deg)						87.518(8)
β (deg)	90.45(3)	102.299(9)	91.99(1)		100.28(2)	88.547(8)
γ (deg)						64.092(8)
V (Å^3)	3379.9	5989.8	7728.9	4978.1	10685(3)	11704.8
μ (Mo Kα_1, mm^{-1})	3.151	3.421	3.691	5.221	5.726	6.887
Z	4	4	4	2	2	2
ρ_c (g cm^{-3})	1.652	1.723	1.801	2.056	2.048	2.357
R indices [$I > 2\sigma(I)$][a]	R1 = 0.0394 wR2 = 0.1067	R1 = 0.0288 wR2 = 0.0747	R1 = 0.0470 wR2 = 0.1068	R1 = 0.0561 wR2 = 0.1445	R1 = 0.0836 wR2 = 0.2236	R1 = 0.0644 wR2 = 0.1491

[a] $R1 = \sum||F_o| - |F_c||/\sum|F_o|$. $wR2 = \{\sum[w(F_o^2 - F_c^2)^2/\sum[wF_o^2]^2\}^{1/2}$.

X-ray Analyses. The selection and mounting of single crystals suitable for X-ray diffraction were carried out by immersing the air-sensitive samples in perfluoropolyetheroil (Riedel de Häen) and mounting the coated crystal on a glass pin set in a goniometer head, the oil setting upon cooling in a flow of N_2. Data were collected on either a Nonius Kappa-CCD diffractometer using COLLECT (Nonius, 1998) software (**6**) or on a STOE IPDS instrument (**1**−**5**) equipped with an imaging plate area detector and a rotating anode. Data were corrected for Lorentz and polarization effects. The SHELXTL (G. M. Sheldrick, Madison, WI) program package was used to solve (direct methods, Cu and Te) and refine the structures. The weighting scheme employed was of the form $w = 1/[\sigma^2(F_o^2) + (a\cdot P)^2 + b\cdot P]$ (a, b = refined variables, $P = {}^1/_3 max(F_o^2, 0) + {}^2/_3 F_c^2$). All structures solved and refined without complications, with the following exceptions: complex **1** was satisfactorily solved and refined in the monoclinic space group P2(1)/c with two crystallographically independent (half) molecules in the asymmetric unit. Due to the similarity of the lengths of axes *b* and *c* and the small value of the angle beta, attempts were made to solve the structure in higher symmetry however these were not successful, as evidenced by the high R(int) (eg. orthorhombic R(int) = 53%). In complex **3**, the ligand P3, the ethyl chains about atoms P1 and P2 and phenyl rings about Te4, Te5, and Te6 were all disordered and a two-site model was satisfactorily refined with 60:40 occupancy. For cluster **4**, a similar two-site model was refined for atoms C1−C6 (50:50 occupancy) and atoms C7−C12 (70:30). Disordered C atoms were refined isotropically. In cluster **6**, atom Te4 was refined anisotropically over two sites with 50:50 occupancy. Complete details of these site disorders are contained in the Supporting Information. A summary of the X-ray determinations is given in Table 1. Figures of complexes **3**−**6** were generated using the Schakal program.[11]

Results and Discussion

Synthesis and Structural Characterization. The use of silyltelluroether reagents offers a facile route into metal−tellurium polynuclear complexes. The $-SiMe_3$ moiety is eliminated readily from the main group metal center when treated with transition metal salts (eq 1).

$$L_nM-X + Te(Ph)SiMe_3 \rightarrow L_nM-TeR + XSiMe_3 \quad (1)$$

Thus when CuCl is dissolved in THF with PMe_3 and treated with $Te(Ph)SiMe_3$, $[Cu_2(\mu\text{-}TePh)_2(PMe_3)_4]$ **1** is isolated in good yield (Scheme 1). The molecular structure of **1** is illustrated in Figure 1 and selected bond lengths and angles are listed in Table 2. Cluster **1** crystallizes in the monoclinic space group $P2(1)/c$ with two independent molecules in the asymmetric unit, each of which resides on a crystallographic inversion center. Although chemically identical, there are marked differences in some of the related bond lengths and angles of the two molecules, illustrating the coordination flexibility of the phenyltellurolate ligands. The Cu centers display pseudo tetrahedral coordination geometry (∠ range from 101.1(1)−121.88(4)°) via a combination of two phosphorus and two tellurium ligands. The μTe−Cu bond distances are similar in both molecules (2.6353(8), 2.6676(7) Å molecule 1; 2.6316(7), 2.6673(9) Å molecule 2) and are typical for bridging tellurolate complexes.[6] The geometry about the Te centers in the two molecules differs significantly. In molecule 1, the angle Cu11−Te11−Cu11A is 63.90(2)° whereas it is 71.63(2)° in molecule 2. This is accompanied with an increase in the nonbonding Cu(I)···Cu(I) distance from 2.806(1) Å in molecule 1 to 3.101(1) Å in molecule 2 and a concomitant rotation of the phenyl rings. Thus in molecule 1, the two *trans* rings line up along the vectors Cu12−Te12 and Cu1B−Te1B respectively, (dihedral angle between planes defined by Cu11−Te11−C11 and Te11−C11−C21 = 2.4°) whereas they are rotated (23.3°) in molecule 2. It is interesting to note that the Cu_2Te_2 arrangements in both molecules of **1** are planar whereas a puckered, butterfly geometry has been reported for the sterically crowded complex $\{Cu[SeC(SiMe_3)_3]PCy_3\}_2$.[12] Oliver et al.[13] have reported a similar Cu_2Se_2 frame with the electrochemical preparation of $[Ph_3PCu(\mu\text{-}SePh)_2Cu(PPh_3)_2]$ that contains both three- and four-coordinate copper

Scheme 1

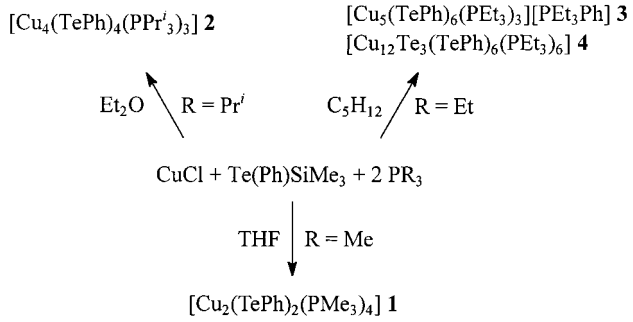

(10) Noviandri, I.; Brown, K. N.; Fleming, D. S.; Gulyas, P. T.; Lay, P. A.; Masters, A. F.; Phillips, L. *J. Phys. Chem. B* **1999**, *103*, 6713−6722.

(11) Keller, E. *SCHAKAL 1999, A Computer Program for the Graphic Representation of Molecular and Crystallographic Models*; Universität Freiburg, 1999.

(12) Bonasia, P. J.; Mitchell, G. P.; Hollander, F. J.; Arnold, J. *Inorg. Chem.* **1994**, *33*, 1797−1802.

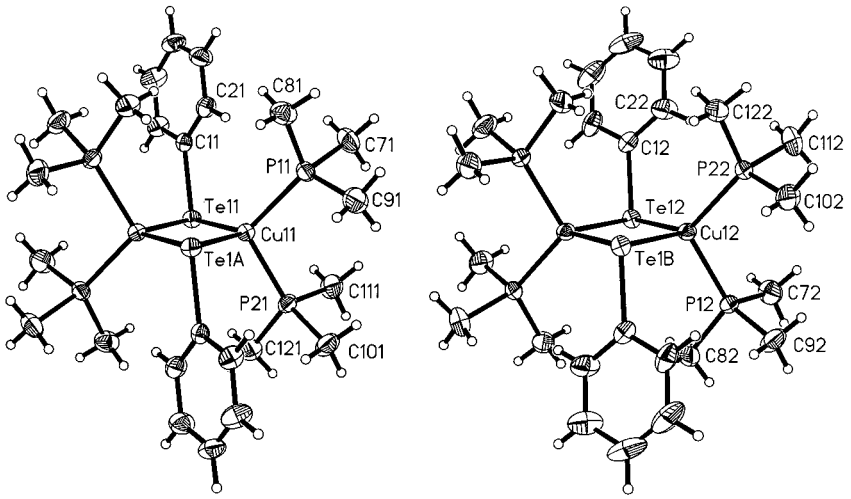

Figure 1. The molecular structure of $[Cu_2(\mu\text{-TePh})_2(PMe_3)_4]$ **1**, illustrating the two crystallographically independent molecules. Thermal parameters are drawn at the 40% probability level.

Table 2. Selected Bond Lengths (Å) and Angles (deg) for $[Cu_2(\mu\text{-TePh})_2(PMe_3)_4]$ **1**, $[Cu_4(\mu\text{-TePh})_4(PPr^i_3)_3]$ **2**, $[Cu_5(TePh)_6(PEt_3)_3][PEt_3Ph]$ **3**, and $[Cu_{12}Te_3(TePh)_6(PEt_3)_6]$ **4**

molecule 1		molecule 2	
	$[Cu_2(\mu\text{-TePh})_2(PMe_3)_4]$ **1**		
Te(11)−C(11)	2.131(4)	Te(12)−C(12)	2.128(4)
Te(11)−Cu(11)	2.6353(9)	Te(12)−Cu(12)	2.6316(7)
Te(11)−Cu(1A)	2.6677(7)	Te(12)−Cu(1B)	2.6672(9)
Cu(11)−P(11)	2.2705(13)	Cu(12)−P(22)	2.2577(11)
Cu(11)−P(21)	2.2705(11)	Cu(12)−P(12)	2.2584(13)
Cu(11)−Te(1A)	2.6677(7)	Cu(12)−Te(1B)	2.6672(9)
Cu(11)−Cu(1A)	2.8063(10)	C(12)−Te(12)−Cu(12)	107.41(11)
C(11)−Te(11)−Cu(11)	107.72(11)	C(12)−Te(12)−Cu(1B)	103.09(11)
C(11)−Te(11)−Cu(1A)	101.10(10)	Cu(12)−Te(12)−Cu(1B)	71.632(19)
P(11)−Cu(11)−P(21)	109.48(5)	P(22)−Cu(12)−P(12)	110.68(4)
P(11)−Cu(11)−Te(11)	121.88(4)	P(22)−Cu(12)−Te(12)	123.83(4)
P(21)−Cu(11)−Te(11)	98.38(4)	P(12)−Cu(12)−Te(12)	101.28(3)
P(11)−Cu(11)−Te(1A)	99.23(4)	P(22)−Cu(12)−Te(1B)	100.78(4)
P(21)−Cu(11)−Te(1A)	112.13(4)	P(12)−Cu(12)−Te(1B)	112.11(4)
Te(11)−Cu(11)−Te(1A)	116.10(2)	Te(12)−Cu(12)−Te(1B)	108.368(19)
	$[Cu_4(\mu\text{-TePh})_4(PPr^i_3)_3]$ **2**		
Te(1)−C(1)	2.124(4)	Te(3)−Cu(4)	2.6510(6)
Te(1)−Cu(1)	2.6251(6)	Te(4)−C(19)	2.132(5)
Te(1)−Cu(3)	2.6254(6)	Te(4)−Cu(4)	2.5554(6)
Te(1)−Cu(4)	2.8420(6)	Te(4)−Cu(3)	3.0557(7)
Te(2)−C(7)	2.124(4)	Te(4)−Cu(1)	3.1484(7)
Te(2)−Cu(2)	2.5734(6)	Cu(1)−P(1)	2.2210(12)
Te(2)−Cu(1)	2.6060(6)	Cu(1)−Cu(4)	2.4843(7)
Te(2)−Cu(4)	2.6680(6)	Cu(2)−P(2)	2.2282(12)
Te(3)−C(13)	2.127(5)	Cu(2)−Cu(4)	2.5337(7)
Te(3)−Cu(2)	2.5960(6)	Cu(3)−P(3)	2.2333(11)
Te(3)−Cu(3)	2.6375(6)	Cu(3)−Cu(4)	2.4822(7)
	$[Cu_5(TePh)_6(PEt_3)_3][PEt_3Ph]$ **3**		
Te(1)−Cu(1)	2.5639(13)	Te(4)−Cu(5)	2.6435(15)
Te(1)−Cu(2)	2.6100(15)	Te(4)−Cu(3)	2.6599(13)
Te(2)−Cu(1)	2.5365(14)	Te(4)−Cu(2)	2.6600(15)
Te(2)−Cu(3)	2.6352(14)	Te(5)−Cu(5)	2.6227(12)
Te(3)−Cu(1)	2.4889(15)	Te(5)−Cu(3)	2.6473(14)
Te(3)−Cu(4)	2.6463(17)	Te(5)−Cu(4)	2.6626(14)
Te(6)−Cu(5)	2.6235(13)	Cu(2)−Cu(5)	2.5869(15)
Te(6)−Cu(2)	2.6497(17)	Cu(3)−Cu(5)	2.6040(17)
Te(6)−Cu(4)	2.6595(16)	Cu(4)−Cu(5)	2.6132(19)
Cu(1)−Cu(5)	2.8909(18)		
	$[Cu_{12}Te_3(TePh)_6(PEt_3)_6]$ **4**		
Te(1)−Cu(1A)	2.6270(13)	Te(2)−Cu(2A)	2.6066(11)
Te(1)−Cu(2)	2.6348(11)	Te(2)−Cu(2)	2.6550(12)
Te(1)−Cu(1)	2.6650(14)	Te(2)−Cu(1)	2.7690(12)

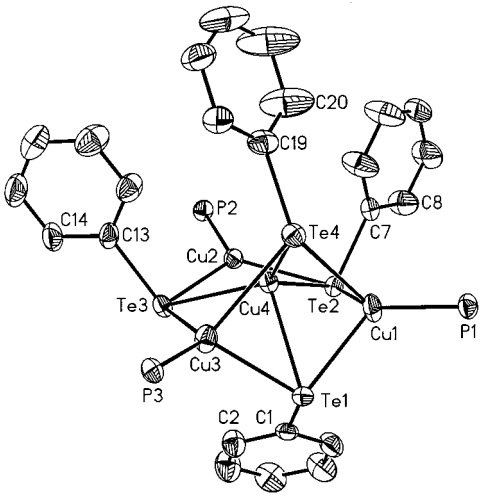

Figure 2. The molecular structure of $[Cu_4(\mu\text{-TePh})_4(PPr^i_3)_3]$ **2**. Thermal parameters are drawn at the 40% probability level. Hydrogen atoms and carbon atoms bonded to the phosphorus centers have been omitted for clarity.

centers with both phenyl rings of the selenolate ligands lying to the same side of the Cu_2Se_2 plane, as observed in $[(Ph_3P)_2Cu(\mu\text{-SPh})_2Cu(PPh_3)_2]$.[14]

A similar reaction for the synthesis of **1** with the larger phosphine[15] PPr^i_3 in diethyl ether leads to the tetranuclear cluster molecule $[Cu_4(\mu_3\text{-TePh})_4(PPr^i_3)_3]$ **2** (Figure 2, Scheme 1). Unlike in **1** where the Cu centers are both four-coordinate, the copper sites in **2** are best described as trigonal planar, with Cu1, Cu3, and Cu4 all displaying a fourth, long contact to tellurium centers (Table 2). The overall geometry of the CuTe core is such that Cu1 and Cu3 asymmetrically cap two faces of the nonbonded Te_4 tetrahedron while Cu2 bridges a Te···Te edge and the only Cu center not bonded to a phosphine ligand (Cu4) lying slightly below a Te_3 face.

An examination of the bonding contacts for the Cu sites in **2** illustrates two symmetrical Cu−Te bonds for (Pr^i_3P)Cu2 (Cu2−Te2 = 2.573(1); Cu2−Te3 = 2.596(1) Å) whereas the other two phosphine bonded centers (Cu1 and Cu3) display two shorter Cu−Te bonds (Cu1−Te1 = 2.625(1); Cu1−Te2 = 2.606(1); Cu3−Te1 = 2.625(1); Cu3−Te3 = 2.638(1) Å) and a markedly long contact to Te4 (Cu1−Te4 = 3.148(1); Cu3−Te4 = 3.056(1) Å). Indeed, the phenyltellurolate ligand Te4 is perhaps best described as "pseudo-terminal" with an exceptionally short Te4−Cu4 bonding distance of 2.555(1) Å. The three additional Cu−Te contacts (Cu4−Te1 = 2.842(1); Cu4−Te2 = 2.668(1); Cu4−Te3 = 2.651(1) Å) are also longer than the former.

Unlike the preparation of **1** and **2**, it did not prove possible to isolate phosphine-stabilized copper−tellurolate complexes with PEt_3 and ethereal solvents, the reaction mixtures invariably producing oily residues. Carrying out the reaction in a less polar solvent (pentane) however, lead to the isolation of $[Cu_5(\mu\text{-TePh})_3(\mu_3\text{-TePh})_3(PEt_3)_3][PEt_3Ph]$ **3** and $[Cu_{12}Te_3(\mu_3\text{-TePh})_6(PEt_3)_6]$ **4** in modest yields (Scheme 1), as the two clusters cocrystallized from the reaction mixture upon standing. The molecular structures of **3** and **4** are illustrated in Figures 3 and 4, respectively. The anionic cluster **3** is comprised of six phenyltellurolate groups and five copper(I) centers, with the

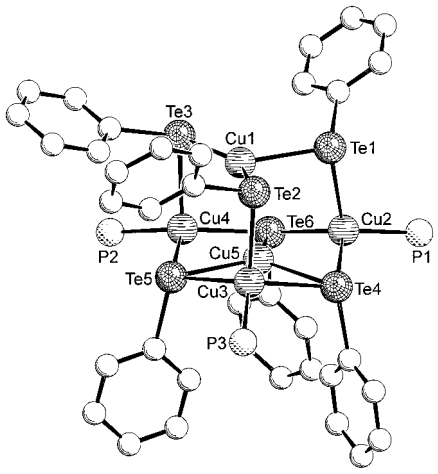

Figure 3. The molecular structure of the anionic cluster $[Cu_5(TePh)_6(PEt_3)_3]^-$ **3**. Carbon atoms about the phosphorus centers and hydrogen atoms have been omitted for clarity.

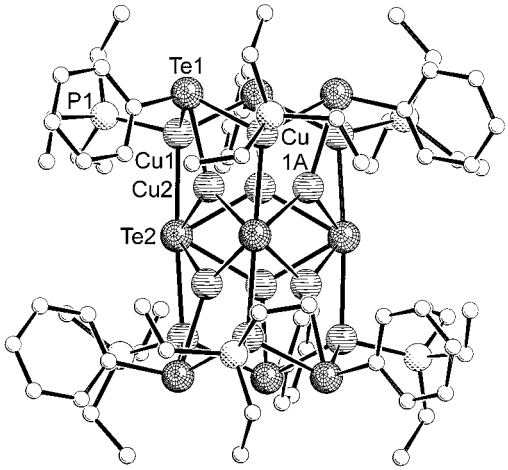

Figure 4. The molecular structure of $[Cu_{12}Te_3(TePh)_6(PEt_3)_6]$ **4** (hydrogen atoms omitted).

$[PEt_3Ph]^+$ cation arising from free phosphine and a phenyl group from TePh centers, as has been observed previously.[6]

In **3** there are three μ_2- (Te1, Te2, Te3) and three μ_3-TePh (Te4, Te5, Te6) ligands defining a distorted octahedral array, with the three PEt_3 bonded Cu centers (Cu2−Cu4) each lying above a deltahedral face. The two remaining three-coordinate Cu centers (Cu1 and Cu5) are both symmetrically bonded to three tellurium ligands (Cu1−Te, 2.489(2)−2.564(1); Cu5−Te, 2.624(1)−2.643(2) Å) with the μ_2-Te−Cu contacts shorter than their μ_3 counterparts. Unlike in **1**, where the μ_3-TePh ligands make two shorter and one longer Te−Cu contacts, the three μ_3-Te(Ph)−Cu bonds are much more symmetric (Cu−Te, 2.629(2)−2.663(2) Å). The smaller PEt_3 ligands (vs PPr^i_3) in **3** thus result in a slightly distorted tetrahedral coordination geometry for Cu2−Cu4, with three roughly equal Cu−Te bond lengths (Table 2). The structure of cluster **3** is closely related to that reported for the neutral complex $[Cu_6(TePh)_6(PEtPh_2)_5]$, with the "additional" $Cu(PR_3)_2$ center bonded to Te1 and Te3.[6]

The second cluster generated with $CuCl{\cdot}PEt_3$, dark green crystals of $[Cu_{12}Te_3(\mu_3\text{-TePh})_6(PEt_3)_6]$ **4**, consists of twelve Cu(I) centers bonded to six μ_3-Te(Ph)$^-$ and three μ_6-Te^{2-} ligands (Figure 4, Table 2), the latter arising from the light-induced generation of $TePh_2$ in the reaction mixture. Indeed, if the reaction is carried in the absence of visible light, clusters **3** and **4** do not form. The structure of **4** is virtually identical to that

(13) Kampf, J.; Kumar, R.; Oliver, J. P. *Inorg. Chem.* **1992**, *31*, 3626−3629.
(14) Dance, I. G.; Guerney, P. J.; Rae, A. D.; Scudder, M. L. *Inorg. Chem.* **1983**, *22*, 2883−2887.
(15) Tolmann, C. A. *Chem. Rev.* **1977**, *77*, 313−348.

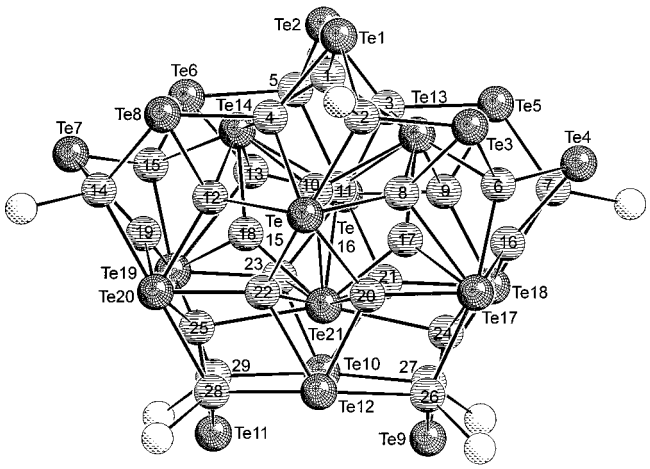

Figure 5. The molecular structure of $[Cu_{29}Te_9(TePh)_{12}(PEt_3)_8]^-$ **5** (carbon atoms omitted). For clarity the copper centers are labeled with numbers only. Phenyltellurolate ligands are labeled Te1−Te12.

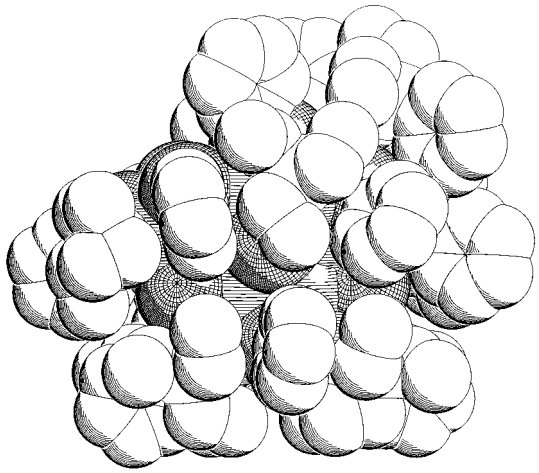

Figure 6. A space filling representation of $[Cu_{29}Te_9(TePh)_{12}(PEt_3)_8][PEt_3Ph]$ **5**.

already described for $[Cu_{12}Te_3(\mu_3\text{-}TePh)_6(PPh_3)_6]$[6] and need not be discussed further here.

Although the solubility of clusters **3** and **4** is limited in hydrocarbon solvents, both are freely soluble in tetrahydrofuran. When a 1:1.5 molar mixture of **3**:**4** is photolyzed (λ cutoff = 320 nm), the reaction mixture gradually darkens to a wine color, and when this is layered with diethyl ether, hair-like crystals of $[Cu_{29}Te_9(\mu_3\text{-}TePh)_{10}(\mu_4\text{-}TePh)_2(PEt_3)_8][PEt_3Ph]$ **5** form in 42% yield. The molecular structure of **5** is illustrated in Figure 5. The highly condensed cluster consists of 29 trigonal planar and tetrahedral copper(I) centers. The bonding contacts for **5** are typical for Cu−Te clusters and are summarized in Table 3. Twelve Ph groups and the eight PEt_3 ligands solubilize the $Cu_{29}Te_{21}$ core, as illustrated with a space-filling model in Figure 6. Indeed, it would appear that the anionic nature of the cluster aids in rendering it much more soluble in THF than related, neutral CuTe complexes.[16,18] With good solubility in THF, it proved possible to explore the electrochemical behavior of **5** (vide infra). The Te_{21} framework in **5** is virtually identical to that reported for the neutral, silver−tellurium cluster $[Ag_{30}(TePh)_{12}Te_9(PEt_3)_{12}]$, that can be synthesized from $Et_3P{\cdot}AgCl$ and a combination of $Te(SiMe_3)_2$ and $Te(Ph)SiMe_3$.[17] The synthesis of **5** from the co-condensation of **3** and **4** arises, in part, from the elimination of $TePh_2$ that can be isolated from the reaction mixture. Although it may be easy to view this reaction as a "2 × 12 Cu + 5 Cu" yields 29 Cu in **5**, the formation of small amounts of brown crystals of $[Cu_{39}(\mu_3\text{-}TePh)_{10}(\mu_4\text{-}TePh)Te_{16}(PEt_3)_{13}]$ **6** from the synthesis of **5** precludes such an oversimplification. The molecular structure of cluster **6** is shown in Figure 7 and a selection of bond lengths is listed in Table 4.

Table 3. Selected Bond Lengths (Å) for $[Cu_{29}Te_9(TePh)_{12}(PEt_3)_8][PEt_3Ph]$ **5**

Te(1)−Cu(4)	2.554(4)	Te(13)−Cu(8)	2.886(5)
Te(1)−Cu(1)	2.661(6)	Te(13)−Cu(10)	2.918(4)
Te(1)−Cu(2)	2.687(5)	Te(13)−Cu(3)	3.080(5)
Te(2)−Cu(3)	2.563(4)	Te(14)−Cu(18)	2.548(3)
Te(2)−Cu(1)	2.628(5)	Te(14)−Cu(1)	2.569(5)
Te(2)−Cu(5)	2.683(5)	Te(14)−Cu(12)	2.704(4)
Te(3)−Cu(6)	2.588(4)	Te(14)−Cu(10)	2.730(4)
Te(3)−Cu(8)	2.595(4)	Te(14)−Cu(13)	2.806(4)
Te(3)−Cu(2)	2.641(4)	Te(14)−Cu(15)	2.896(5)
Te(4)−Cu(6)	2.561(4)	Te(14)−Cu(11)	3.040(4)
Te(4)−Cu(16)	2.632(4)	Te(14)−Cu(4)	3.074(5)
Te(4)−Cu(7)	2.642(4)	Te(15)−Cu(8)	2.555(4)
Te(5)−Cu(3)	2.644(5)	Te(15)−Cu(10)	2.633(4)
Te(5)−Cu(7)	2.647(4)	Te(15)−Cu(4)	2.686(4)
Te(5)−Cu(9)	2.662(4)	Te(15)−Cu(22)	2.741(4)
Te(6)−Cu(13)	2.606(4)	Te(15)−Cu(20)	2.794(4)
Te(6)−Cu(15)	2.606(4)	Te(15)−Cu(2)	2.811(4)
Te(6)−Cu(5)	2.642(5)	Te(15)−Cu(12)	2.949(4)
Te(7)−Cu(15)	2.560(4)	Te(16)−Cu(13)	2.583(4)
Te(7)−Cu(19)	2.622(4)	Te(16)−Cu(11)	2.612(4)
Te(7)−Cu(14)	2.657(5)	Te(16)−Cu(3)	2.640(4)
Te(8)−Cu(4)	2.625(5)	Te(16)−Cu(21)	2.724(4)
Te(8)−Cu(14)	2.652(5)	Te(16)−Cu(23)	2.761(4)
Te(8)−Cu(12)	2.669(4)	Te(16)−Cu(5)	2.808(5)
Te(9)−Cu(24)	2.591(4)	Te(16)−Cu(9)	3.034(4)
Te(9)−Cu(27)	2.621(5)	Te(17)−Cu(20)	2.597(4)
Te(9)−Cu(26)	2.665(5)	Te(17)−Cu(6)	2.679(4)
Te(10)−Cu(23)	2.623(4)	Te(17)−Cu(16)	2.719(4)
Te(10)−Cu(27)	2.681(5)	Te(17)−Cu(26)	2.728(4)
Te(10)−Cu(29)	2.732(5)	Te(17)−Cu(24)	2.750(4)
Te(10)−Cu(21)	2.838(4)	Te(17)−Cu(17)	2.765(4)
Te(11)−Cu(25)	2.594(4)	Te(17)−Cu(8)	3.061(4)
Te(11)−Cu(29)	2.641(5)	Te(18)−Cu(16)	2.562(4)
Te(11)−Cu(28)	2.645(5)	Te(18)−Cu(21)	2.585(4)
Te(12)−Cu(20)	2.619(4)	Te(18)−Cu(9)	2.622(4)
Te(12)−Cu(28)	2.682(5)	Te(18)−Cu(24)	2.673(4)
Te(12)−Cu(26)	2.723(5)	Te(18)−Cu(27)	2.790(4)
Te(12)−Cu(22)	2.843(4)	Te(18)−Cu(7)	2.804(4)
Te(13)−Cu(17)	2.548(3)	Te(19)−Cu(23)	2.580(4)
Te(13)−Cu(1)	2.580(5)	Te(19)−Cu(15)	2.684(4)
Te(13)−Cu(9)	2.736(4)	Te(19)−Cu(25)	2.707(4)
Te(13)−Cu(11)	2.759(4)	Te(19)−Cu(19)	2.720(4)
Te(13)−Cu(6)	2.838(5)	Te(19)−Cu(29)	2.724(4)
Te(19)−Cu(18)	2.770(4)	Te(21)−Cu(17)	2.589(4)
Te(19)−Cu(13)	3.061(4)	Te(21)−Cu(22)	2.720(4)
Te(20)−Cu(19)	2.563(4)	Te(21)−Cu(21)	2.739(4)
Te(20)−Cu(22)	2.568(4)	Te(21)−Cu(20)	2.860(4)
Te(20)−Cu(12)	2.640(4)	Te(21)−Cu(23)	2.860(4)
Te(20)−Cu(25)	2.664(4)	Te(21)−Cu(24)	3.001(4)
Te(20)−Cu(28)	2.773(5)	Te(21)−Cu(11)	3.035(4)
Te(20)−Cu(14)	2.822(5)	Te(21)−Cu(25)	3.093(4)
Te(21)−Cu(18)	2.577(4)	Te(21)−Cu(10)	3.135(4)

The structure of the copper−telluride cluster **6** is perhaps best described as being related to that of **5** that has undergone "skeletal expansion". Although there are but 11 $Te(Ph)^-$ moieties in **6** (vs12 in **5**), there are 16 Te^{2-} centers distributed in the cluster core. The latter Te sites are arranged to yield a (nonbonded) tri-capped centered icosahedron (Figure 8), such deltahedral arrangements a common characteristic of high-nuclearity, spherical $[Cu_xTe_y(PR_3)_z]$ clusters.[18] Also similar to such Cu−Te condensed systems, the Cu:Te:Te(Ph) ratio in **6** is such that it is not possible to assign a +1 oxidation state to the copper centers. Noteworthy with the structures of the

(16) Semmelmann, M.; Fenske, D.; Corrigan, J. F. *J. Chem. Soc., Dalton Trans.* **1998**, 2541−2545.
(17) Corrigan, J. F.; Fenske, D. *Chem. Commun.* **1997**, 1837−1838.
(18) Corrigan, J. F, Balter, S.; Fenske, D. *J. Chem. Soc., Dalton Trans.* **1996**, 729−738.

Table 4. Selected Bond Lengths (Å) for $[Cu_{39}(TePh)_{11}Te_{16}(PEt_3)_{13}]$ **6**

Te(1)−Cu(4)	2.5648(16)	Te(13)−Cu(9)	2.6440(16)	Te(12)−Cu(9)	2.6813(15)	Te(18)−Cu(27)	2.7936(16)
Te(1)−Cu(6)	2.6326(16)	Te(13)−Cu(1)	2.6901(16)	Te(12)−Cu(2)	2.7348(16)	Te(18)−Cu(30)	2.8159(16)
Te(1)−Cu(8)	2.6859(17)	Te(13)−Cu(12)	2.7679(15)	Te(12)−Cu(5)	2.7799(16)	Te(18)−Cu(19)	3.0011(16)
Te(2)−Cu(7)	2.6379(15)	Te(13)−Cu(5)	3.0017(16)	Te(12)−Cu(1)	2.7881(17)	Te(18)−Cu(16)	3.0035(17)
Te(2)−Cu(3)	2.6395(17)	Te(14)−Cu(19)	2.5494(16)	Te(12)−Cu(7)	2.9170(16)	Te(19)−Cu(4)	2.6737(17)
Te(2)−Cu(2)	2.6922(17)	Te(14)−Cu(21)	2.5570(16)	Te(13)−Cu(16)	2.5468(15)	Te(19)−Cu(18)	2.6786(16)
Te(3)−Cu(5)	2.6195(16)	Te(14)−Cu(10)	2.6563(15)	Te(13)−Cu(15)	2.5594(15)	Te(19)−Cu(20)	2.7130(16)
Te(3)−Cu(3)	2.6362(17)	Te(14)−Cu(2)	2.7112(16)	Te(19)−Cu(31)	2.7365(16)	Te(24)−Cu(25)	2.6439(16)
Te(3)−Cu(1)	2.6887(16)	Te(14)−Cu(13)	2.7321(16)	Te(19)−Cu(8)	2.7586(17)	Te(24)−Cu(36)	2.6517(16)
Te(4)−Cu(17)	2.6349(16)	Te(14)−Cu(7)	2.8059(17)	Te(19)−Cu(28)	2.7610(16)	Te(24)−Cu(21)	2.6570(16)
Te(4)−Cu(11)	2.6459(17)	Te(15)−Cu(5)	2.5542(15)	Te(19)−Cu(17)	2.7778(17)	Te(24)−Cu(13)	2.6807(16)
Te(4)−Cu(4)	2.6793(17)	Te(15)−Cu(7)	2.6001(16)	Te(20)−Cu(24)	2.5771(16)	Te(24)−Cu(30)	2.7003(17)
Te(5)−Cu(22)	2.6336(16)	Te(15)−Cu(19)	2.6541(17)	Te(20)−Cu(27)	2.5975(16)	Te(24)−Cu(35)	2.8712(16)
Te(5)−Cu(11)	2.6643(17)	Te(15)−Cu(16)	2.6823(15)	Te(20)−Cu(12)	2.6880(15)	Te(24)−Cu(26)	2.8851(16)
Te(5)−Cu(15)	2.6875(15)	Te(15)−Cu(24)	2.7776(16)	Te(20)−Cu(16)	2.7012(15)	Te(25)−Cu(35)	2.5626(16)
Te(6)−Cu(26)	2.6194(15)	Te(15)−Cu(3)	2.8433(16)	Te(20)−Cu(29)	2.7464(17)	Te(25)−Cu(31)	2.5813(16)
Te(6)−Cu(14)	2.6654(16)	Te(16)−Cu(6)	2.6023(15)	Te(20)−Cu(32)	3.0624(19)	Te(25)−Cu(26)	2.5837(15)
Te(6)−Cu(21)	2.6780(17)	Te(16)−Cu(23)	2.6350(15)	Te(21)−Cu(24)	2.5827(16)	Te(25)−Cu(20)	2.7397(17)
Te(7)−Cu(20)	2.6057(16)	Te(16)−Cu(9)	2.6663(15)	Te(21)−Cu(30)	2.6059(15)	Te(25)−Cu(14)	2.7992(16)
Te(7)−Cu(8)	2.6696(17)	Te(16)−Cu(18)	2.6882(17)	Te(21)−Cu(19)	2.6455(15)	Te(25)−Cu(38)	2.8055(17)
Te(7)−Cu(14)	2.6794(17)	Te(16)−Cu(17)	2.7831(16)	Te(21)−Cu(13)	2.7041(16)	Te(26)−Cu(25)	2.6444(15)
Te(8)−Cu(28)	2.6561(16)	Te(16)−Cu(22)	2.7980(15)	Te(21)−Cu(32)	2.7289(16)	Te(26)−Cu(23)	2.6453(16)
Te(8)−Cu(31)	2.6792(15)	Te(16)−Cu(15)	2.8121(16)	Te(21)−Cu(29)	2.9604(18)	Te(26)−Cu(18)	2.6866(16)
Te(8)−Cu(37)	2.7056(17)	Te(16)−Cu(4)	2.9071(17)	Te(22)−Cu(33)	2.5534(14)	Te(26)−Cu(33)	2.7950(16)
Te(8)−Cu(38)	2.7193(17)	Te(17)−Cu(25)	2.6351(15)	Te(22)−Cu(22)	2.6040(15)	Te(26)−Cu(28)	2.8096(15)
Te(9)−Cu(33)	2.6417(15)	Te(17)−Cu(6)	2.6481(17)	Te(22)−Cu(28)	2.6055(16)	Te(26)−Cu(31)	2.8098(17)
Te(9)−Cu(37)	2.6470(16)	Te(17)−Cu(18)	2.6613(16)	Te(22)−Cu(17)	2.6163(15)	Te(26)−Cu(36)	2.8176(17)
Te(9)−Cu(34)	2.6477(15)	Te(17)−Cu(10)	2.6786(16)	Te(22)−Cu(37)	2.8246(16)	Te(26)−Cu(35)	2.8242(17)
Te(10)−Cu(32)	2.6398(16)	Te(17)−Cu(20)	2.7022(16)	Te(22)−Cu(11)	2.8254(16)	Te(26)−Cu(34)	2.8432(16)
Te(10)−Cu(29)	2.6431(17)	Te(17)−Cu(26)	2.7565(17)	Te(23)−Cu(23)	2.6312(15)	Te(27)−Cu(32)	2.5412(16)
Te(10)−Cu(39)	2.6563(19)	Te(17)−Cu(21)	2.8285(16)	Te(23)−Cu(34)	2.6540(17)	Te(27)−Cu(36)	2.5432(17)
Te(11)−Cu(36)	2.6219(17)	Te(18)−Cu(23)	2.6463(14)	Te(23)−Cu(15)	2.6700(16)	Te(27)−Cu(34)	2.5432(15)
Te(11)−Cu(35)	2.6367(15)	Te(18)−Cu(25)	2.6547(16)	Te(23)−Cu(12)	2.7161(16)	Te(27)−Cu(27)	2.7381(17)
Te(11)−Cu(38)	2.6553(17)	Te(18)−Cu(9)	2.6548(15)	Te(23)−Cu(27)	2.7357(15)	Te(27)−Cu(30)	2.7418(15)
Te(12)−Cu(6)	2.5871(16)	Te(18)−Cu(24)	2.6634(15)	Te(23)−Cu(22)	2.8180(15)	Te(27)−Cu(39)	2.7588(17)
Te(12)−Cu(10)	2.6779(16)	Te(18)−Cu(10)	2.6685(15)	Te(23)−Cu(33)	2.9078(16)		

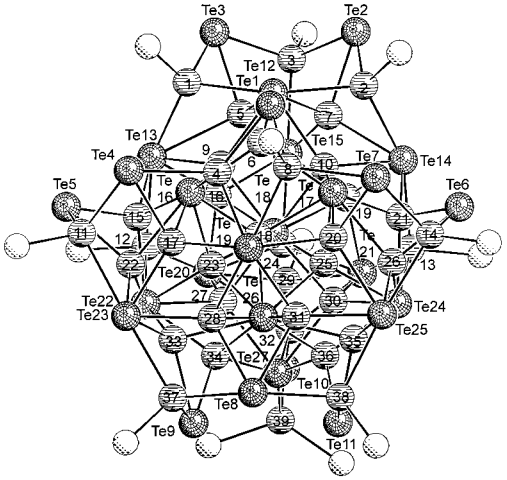

Figure 7. The molecular structure of the $[Cu_{39}(TePh)_{11}Te_{16}(PEt_3)_{13}]$ 6 (carbon atoms omitted). For clarity the copper centers are labeled with numbers only. Phenyltellurolate ligands are labeled Te1−Te11.

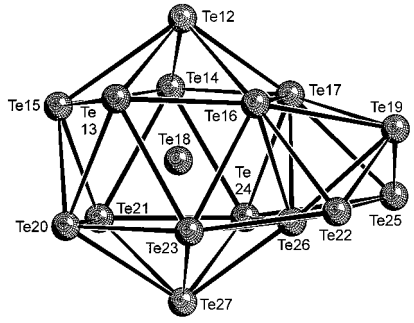

Figure 8. The (nonbonded) Te framework of the telluride ligands in **6**.

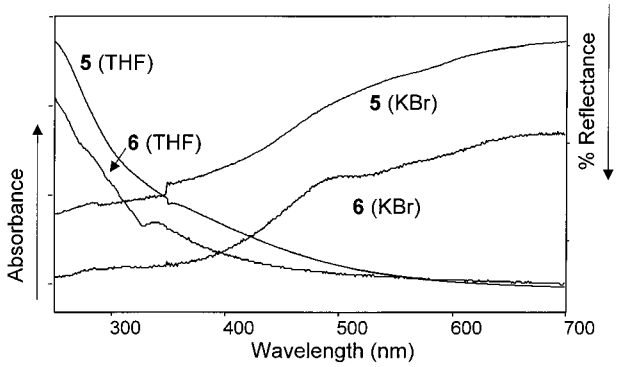

Figure 9. Solution and solid-state (diffuse reflectance) UV−vis spectra for **5** and **6**.

nanoclusters **5** and **6** is that they bear no resemblance to those reported for triethylphosphine/alkyltellurolate/telluride/copper clusters,[18,19] clearly demonstrating the effect that the carbon substituents on tellurium exert on controlling product formation.

UV−Vis Spectroscopy and Cyclic Voltammetry. The UV−vis solution spectrum of **5** in THF displays a broad featureless absorption, with an onset of ∼520 nm and no discernible maximum (Figure 9). The solid-state (diffuse reflectance, in KBr) spectrum displays a similar profile, although there is a weak maximum observed at ∼570 nm. The solution spectrum for **6** is similar to that observed for **5** (Figure 9) with an onset of absorption at $\lambda \sim 600$ nm. The diffuse reflectance spectrum UV−vis spectrum of **6** in KBr shows an additional feature, with

(19) Fenske, D.; Zhu, N. Y. *J. Cluster Sci.* **2000**, *11*, 135−151.

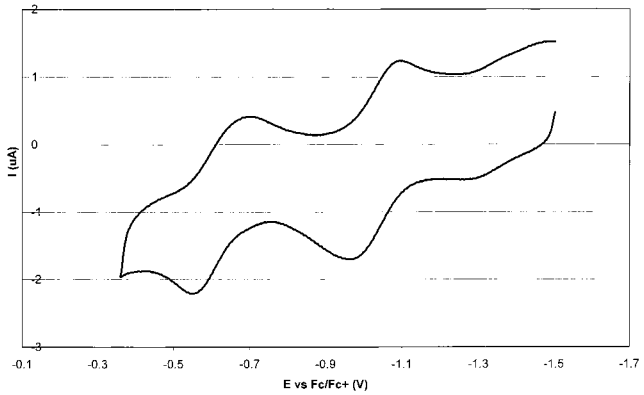

Figure 10. The cyclic voltammogram for **5** in THF (1 mM) with 0.1 M $[NBu_4][BF_4]$ (100 mV/s).

a clearly defined absorption band at 520 nm. Similar absorption profile characteristics have been reported recently for high-nuclearity copper telluride clusters, and the lower energy bands have been attributed to the delocalized bonding in such nanometer sized particles.[2a]

The good solubility of the anion **5** permitted an electrochemical analysis to be performed. An electrochemical cell was prepared by dissolving 1 or 2 mM Cu_{29} in dry THF containing 0.1−0.2 M $[Bu_4N][BF_4]$ as an electrolyte, to give a red−wine solution. A three-electrode setup was used as described in the Experimental Section. Cyclic voltammograms (CV's) were obtained by scanning between −1 to 0.8 V at scan rates varying from 0.05 V/s to 0.5 V/s. Figure 10 shows a representative CV measured at 0.2 V/s showing two single electron processes that are chemically reversible on these time scales. These redox processes are assigned to the reversible anodic oxidation of $[Cu_{29}]^-$ to the neutral Cu_{29} complex and subsequent further oxidation of the neutral complex to the corresponding cation. The standard potentials of these two processes are −1.02 and −0.64 ±0.01 V versus the ferrocene/ferrocinium redox couple, respectively. Attempts to isolate either of the two oxidized species using appropriate counterions have yet to prove successful. While the neutral complex is stable under these conditions over the time scale of the experiment, the loss of some of the chemical reversibility of the cation at slower scan rates suggests that there is a competing chemical process that is occurring.

Conclusions

A series of trialkylphosphine-stabilized copper−tellurolate cluster complexes has been prepared using the silylated reagent $Te(Ph)SiMe_3$. We have shown that controlled condensation of low nuclearity clusters can be achieved using photolysis to promote the elimination of $TePh_2$, leading to the generation of nanometer sized copper−tellurium frameworks.

Acknowledgment. We are grateful to the Natural Sciences and Engineering Research Council of Canada and the University of Western Ontario's ADF program for supporting this research. Dr. Nicholas J. Taylor (University of Waterloo, Canada) is thanked for discussions regarding the X-ray refinement of **5**. We also acknowledge the Canada Foundation for Innovation and the Ontario Research and Development Challenge Fund for equipment funding. J.F.C. thanks Prof. Dieter Fenske (Universität Karlsruhe) for providing access to facilities for X-ray data collection.

Supporting Information Available: X-ray crystallographic files in CIF format for the structure determinations of **1**−**6**. This material is available free of charge via the Internet at http://pubs.acs.org.

IC001260K